Received: 21 February 2024 | Revised: 8 October 2025 | Accepted: 3 November 2025

DOI: 10.1002/esp.70203

RESEARCH ARTICLE

ESPL WILEY

Formation of repeating bar-flat bedforms in ephemeral gravel bed channels: 1. Field observations

Jonathan B. Laronne[1,2,3] | Tal Cohen[1] | D. Mark Powell[4] | Michael Dorman[3] | Annunziato Siviglia[5] | Marco Tubino[5] | Gabriele Massera[5] | Ian Reid[6]

[1]Department of Earth & Environmental Sciences, Ben Gurion University of the Negev, Beer Sheva, Israel

[2]Dead Sea Arava Science Center, Dead Sea, Israel

[3]Department of Environmental, Geoinformatics and Urban Planning Sciences, Ben Gurion University of the Negev, Beer Sheva, Israel

[4]School of Geography, Geology and the Environment, University of Leicester, Leicester, UK

[5]Department of Civil, Environmental and Mechanical Engineering, University of Trento, Trento, Italy

[6]Department of Geography & Environment, Loughborough University, Loughborough, UK

Correspondence
Jonathan B. Laronne, Department of Earth & Environmental Sciences, Ben Gurion University of the Negev, Beer Sheva, Israel.
Email: john@bgu.ac.il

Funding information
The project was funded in part by the Israel Science Foundation Grant 832/14. A. Siviglia and M. Tubino acknowledge the Italian Ministry of Education, Universities and Research (MUR) in the framework of the project DICAM-EXC (Departments of Excellence 2023-2027, grant L232/2016).

Abstract

Repeating fluvial macroforms are ubiquitous. The streamwise alternation of steeper, coarse-grained, cobble/pebble bars and near-horizontal, fine-grained, sand/granule flats is characteristic of upland, single-thread, dryland channels. We have monitored the rate of formation of a bar-flat sequence by flash floods, noting the disposition and extent of each macroform as they evolve. To accomplish this, the bed material of a straight reach of the Nahal Yatir in the northern Negev Desert, Israel, was thoroughly mixed to a depth of 0.5 m with the aid of a mini excavator, obliterating a well-formed sequence of bars and flats. The ten flow events of two succeeding rain seasons were recorded, as were the changing topography and textural roughness of the bed following each complete post-flood dewatering. Embryonic flats, texturally like those present before disturbance, formed under the first flow event, occupying a fifth of the total length of the flats that had existed in the reach before experimental disturbance. Their length increased and their inclination decreased with each flow event, returning to the natural, pre-disturbed, aggregated length within two rain seasons. Restoration of the pre-disturbance bar-flat sequence was almost complete, the location of bars differing only marginally in places. Resemblance with the natural original was high, reflecting the sedimentary dynamism of desert flash floods. A mechanism that models and explains the formation and stability of these macroform sequences is developed in a companion paper.

KEYWORDS
bar-flat bedform, bedload, flash-flood, gravel-bed river, macroform, SfM

1 | INTRODUCTION

The beds of single-thread, upland, ephemeral channels are characterized by a sequence of bars and flats (Powell et al., 2012; Reid & Laronne 1995). These are reminiscent of the riffle-pool sequence in perennial mountain rivers (Chin & Wohl, 2005; Clifford, 1993; Montgomery & Buffington, 1997; Richards, 1976), but they possess unique characteristics that distinguish them from their perennial counterparts. Although similarly, the bars are relatively steep, they are only very lightly armoured, if armoured at all (Laronne et al., 1994). Flats are much finer-grained than neighbouring bars and their surface is generally planar, contrasting with the typical concave-up, longitudinal profile of pools in perennial channels (Powell et al., 2012). Bars in these ephemeral channels, be they single or multi-thread, contain most of the coarse surface clasts (Hassan, 2005; Storz-Peretz & Laronne, 2013, 2018). In contrast, flats are typically sand-granule-pebble mixtures, with occasional over-passing coarser clasts, and, importantly, they are always inversely graded, exhibiting no armour.

What are the conditions that give rise to alternating bedforms in gravel-bed rivers, both ephemeral and perennial? Their variety reflects the complex interaction between flowing water and the sediment bed, and the control exerted by river shape, and local and hydrological factors affecting boundary conditions. Short- and long-term variations in sediment supply have been shown to be important (Buffington & Montgomery, 1999). Some have argued that the alternation reflects meander planform and is a sedimentary adjustment to local slope (Chin, 2002). Different forcing mechanisms (hydraulic, granular interaction, random drivers) have been proposed to explain the formation of step-pool morphologies in high-gradient streams (Golly et al., 2019). As for fluvial bars, while channel curvature has been recognized as the main cause of the rhythmic sequences of riffles and pools observed in meandering rivers, the spontaneous development of migrating alternate bars in straightened river reaches has been explained as a consequence of the inherent instability of the sediment bed, where the major destabilizing effect is friction, while the downslope pull of gravity on bedload plays a stabilizing role (Callander, 1969; Colombini et al., 1987; Parker, 1976). An analogous instability mechanism has been found to drive the formation of small-scale bedforms - such as ripples, dunes and antidunes (Engelund, 1970; Hayashi, 1970; Kennedy, 1963; Richards, 1980).

Various repetitive patterns due to grain sorting effects have been investigated. Venditti et al. (2017) have provided a detailed evaluation of gravel bedforms and fine-grained patches. The formation of fine-grained bedload sheets has been described by Whiting et al. (1988) and Recking et al. (2009), as have sand-rich gravel bedforms by Kuhnle et al. (2006). More recently, several drivers have been proposed for the persistence of fine-grained bed patches (Stark et al., 2025). Coarse-grained, steep macroforms have been shown to persist as a function of armouring and stabilization of the bed (Whittaker & Jaeggi, 1982). However, the mechanisms that lead to the formation and stability of alternating bar-flat sequences in ephemeral channels remain undetermined.

Here, we report on a field experiment, the aims of which were to observe and characterize the formation of a bar-flat sequence under flash flood flows. We have asked the following: were a bar-flat sequence to be destroyed through artificial homogenization of the bed material, does it re-form? and, if so, how quickly? What is the minimum number and the magnitude of bedload transporting events that bring about this re-formation? Does the sequence re-form exactly as it was originally or just similarly?

In a companion paper, we develop a mechanistic model that accounts for the formation of a bar-flat sequence.

2 | RESEARCH AREA

Our research has been conducted in the Nahal Yatir, a 4th order tributary that drains 19 km^2 of the southern Hebron Hills towards the Nahal Beer Sheva and, thereafter, the Nahal Bsor and, eventually but only occasionally, the Mediterranean (Figure 1). The upper part of the catchment is underlain by Turonian Bina limestone, while the lower parts lie in Senonian Menuha chalk, which includes beds of Meshash chert, and Miocene Yatir conglomerate. Quaternary loess is ubiquitous, but its thickness varies considerably from a few decimetres on interfluves to several metres in valley bottoms (Sneh & Avni, 2008). This is a transitional phytogeographic area between Mediterranean and desert vegetation, with few shrubs on the hillslopes and dense shrubs lining channel banks (Danin et al., 1998). Much of the catchment remains devoid of vegetation cover for most of the year. However, grasses germinate after the first winter rains. A pine woodland was planted in the upper catchment in the 1960s, and scattered Eucalyptus groves have been added more recently.

This semi-arid area is part of the Northern Negev, Israel, where very localized and intense rain events are delivered by Red Sea monsoonal troughs (Shentsis et al., 2012), and longer-lasting and less intense events are brought by Mediterranean frontal systems (Kahana et al., 2002), both storm types arriving between October and April. Mean annual rainfall is 220–280 mm. However, evaporation is considerable, with a potential of > 2,000 mm/a, so that, between rain events, the surface-crusted, largely bare, loessial soils become hydrophobic. Consequently, infiltration-excess runoff is quickly generated by subsequent storms (Assouline & Ben-Hur, 2006; Ben-Hur et al., 1985; Yair & Kossovsky, 2002).

The duration of channel flow varies, depending on rainfall pattern, but is typically only a few hours, with rare longer exceptions (Yair & Kussovsky, 2002). The channel is, therefore, dry for most of the year, including most of the winter. Flow events characteristically have fast rise times (< 10 min), arriving as flood bores, the first of which invariably overrides a dry river bed (Reid, Laronne, & Powell, 1995; Reid et al., 1998).

The Yatir is a small gravel-bed stream with an average width of 1.6 m and a bed slope of 0.01 at the study site. Its modest dimensions were important for our plans, in part because of our intention to reorganize a large volume of bed material over a reasonably long reach, but also because of the need to obtain comprehensive, detailed documentation of channel bed evolution over the entire study reach during succeeding rain seasons.

As important, the channel bed prior to treatment was punctuated by moderately coarse, channel-wide, gravel bars and intervening 'flats' of finer gravel and sand, as exemplified by the nearby Nahal Anim (Figure 2) and typical of single-thread, coarse-grained stream beds in the Negev (Powell et al., 2012). Previous studies have shown that flats in the Yatir bed are un-armoured – indeed, they have an inverse grading – while bars have a neutral grading (Barzilai, 2012; Laronne et al., 1994; Reid & Laronne, 1995). The absence of armour development has been suggested to reflect the ample supply of sediment from the sparsely vegetated catchment and the rapid recession of flash flood hydrographs, the latter giving insufficient time to promote armour development (Hassan et al., 2006; Reid & Laronne, 1995; Storz-Peretz et al., 2016).

A prior, 3-D survey of bars and flats in the Yatir (Barzilai, 2012) had demonstrated that: (i) there is no significant difference between the lengths of the flats and the bars; (ii) the depth of finer-grained flat material is in the range 8–24 cm (mean = 14.5 cm, SD = 4.8 cm) and is independent of local channel width, surface slope and length of the flats; (iii) cross-sections of flat sediments show that their base is invariably concave-up; and (iv) a flat can be represented by a simple, elongate saucer, filled with finer-grained sediments and feathering onto adjacent bars both up- and downstream, reminiscent of pools that infill with fine sediment under a regime of high sediment supply in perennial systems (Lisle & Hilton, 1999).

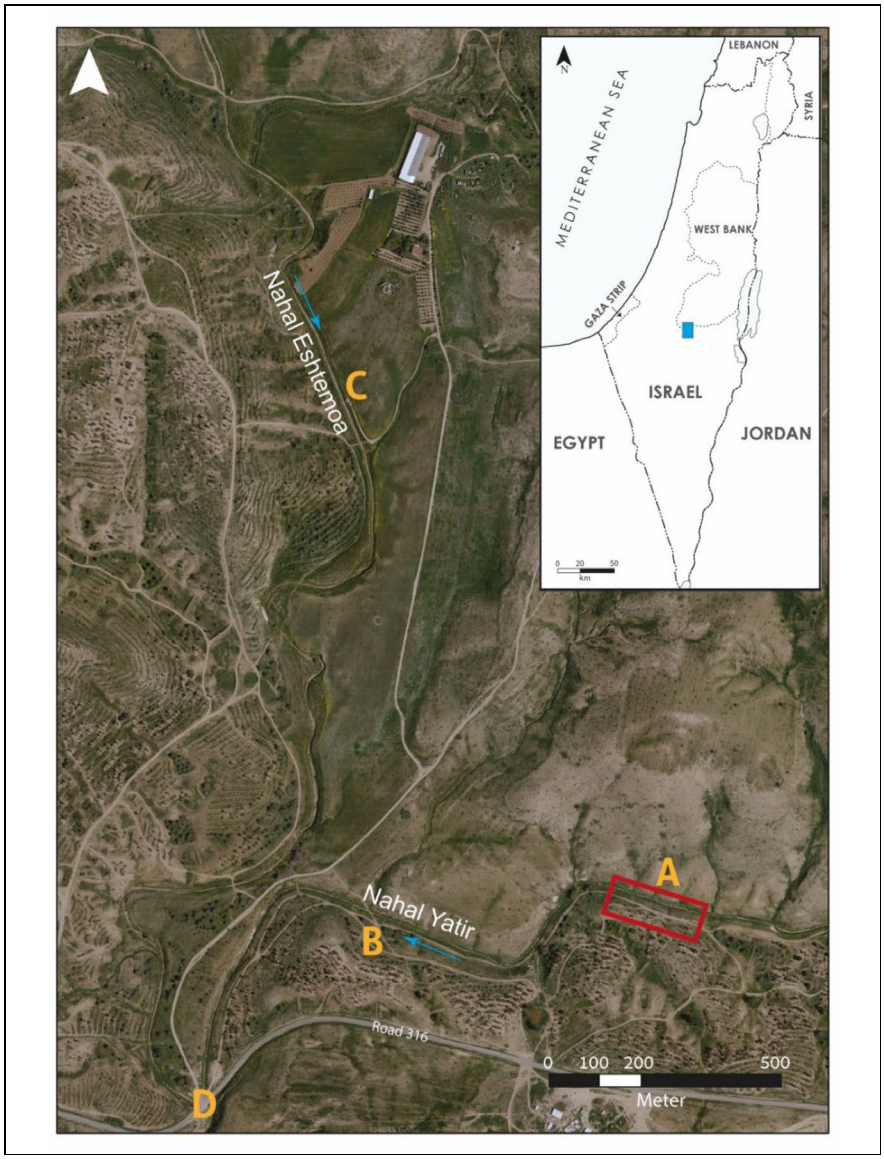

FIGURE 1 The study reach of Nahal Yatir (A) located upstream of the current water depth monitoring site and former bedload sampling station (B); the current bedload sampling station on the Nahal Eshtemoa (C); the Yatir-Eshtemoa confluence (D). Inset: the location of the Yatir catchment (blue box) in the Northern Negev.

FIGURE 2 Sequences of flats (F) and bars B) along two reaches of the Nahal Anim located just east of the Nahal Yatir. A similar sequence typifies all neighbouring upland channels. The blue arrows indicate flow direction.

3 | METHODS

To achieve our research objectives, we deconstructed the bedforms of a reach of the channel, homogenizing the top 0.5 m of bed material (c. 90 m^3, weighing c. 150 Mg) as thoroughly as is feasible and leaving it as planar as possible. The changes in surface morphology and sedimentology were then documented over two years as successive flashfloods of varying magnitude impinged on the initially artificial bed. No other changes were made to the channel: its sidewalls and the often dense, thorny, bank vegetation were left intact.

We chose a straight, 108 m long reach in which bedforms were delimited by eye, identifying four bars, four flats and three transitional zones that exhibit a mix of bar and flat characteristics.

Imagery of the dry post-flood bed was captured through repeat photography (Carrivick et al., 2016). This was achieved by walking the channel while operating a Panasonic Lumix DMC TZ60 4.3 mm camera gimbled on the end of a 1.9 m rod in order to ensure the principal axis of the lens was vertical (Smith & Vericat, 2015). For each survey, 40 × 40 cm wooden targets (first flood season) and cement targets (second flood season) were located at appropriate points on the banks adjacent to the channel throughout the reach. Their locations were established with a total station. The Panasonic Image App facilitated ~ 80% overlap of sequential images so that every portion of the bed appeared in three consecutive images (*cf* Westoby et al., 2012). To avoid distortion due to variations in illumination, photography was undertaken either just prior to sunrise, or, most often, in the late afternoon when the entire channel bed was in shade. The study reach was photographed in its original state in October 2016 and, subsequently, after every flow event except one, which was followed too quickly by the next to allow field operations. Monitoring continued until the end of the second flood season. The longitudinal slope of each macroform was determined in detail by a total station before and after each flow event. Detrending of each macroform's longitudinal slope was achieved by generating a Digital Elevation Model (DEM).

Field data were processed into a height grid with a resolution of 0.2–0.7 cm and orthophotos produced using the Agisoft Photoscan software. Data processing was undertaken in several main steps:

1. Alignment of the images (*cf* Westoby et al., 2012);
2. Geographic alignment was undertaken by loading the target locations with target identification; association with location was performed manually (cf. Smith & Vericat, 2015). Some of the targets were not used to construct the point cloud and were defined as check points.
3. Condensation of the initial point cloud into a dense point (*cf* Dietrich, 2014). The calculation of the average error between the height grid and the total station measurement was performed for both types of target placed in the field (Check points, Ground control points). For each location, the maximum error, minimum error and the root mean square error (RMSE) were calculated:

$$\sqrt{\frac{1}{n-1}\sum_{i=1}^{n}(\hat{y}-y_i)^2},$$

where n is the total number of observations, $\hat{y}$ is the expected value from a linear regression of the values measured by the total station against the value obtained at the height gauge and y_i is the value obtained by the SfM (Taylor, 1997).

The elevation grid was processed for a statistical analysis of the frequency distribution of elevations in each stream bed unit to assess the degree of roughness (Table S2; Supplement 2). The processing was carried out consistently during the preparation phase, after the controlled homogenization of the streambed and following almost all flood events. The purpose of processing the elevation grid was to generate a statistical analysis of elevations which characterize the surface roughness (to which the surficial grain sizes are supposedly correlated) and thereby distinguish between the appearance of a bar and a flat (do Prado et al., 2025; Storz-Peretz et al., 2016).

The following procedure was undertaken to determine the temporal variation of the roughness of flats and, separately, of bars, each selected visually (Figure 3). Three different scales of topography exist in the resulting elevation profiles. The macro scale is that of the general channel slope, expressed as a 1 m difference between the upstream and downstream sections of the study reach. The intermediate scale includes the local topography of the channel macroforms, with slopes ranging from 3.6 to −0.1%. The microscale is associated with the roughness of particles on the bed surface.

To distinguish surface roughness, detrending was performed on all segments marked in each of the elevation grids. The detrending created a reduction between the slope of the selected segment and the original elevation grid and, in effect, 'eliminated' the effect of the channel slope and the local topography. After subtracting the surface slope from the original elevation grid, an aligned elevation grid was obtained that represents the roughness scale. The negative values in

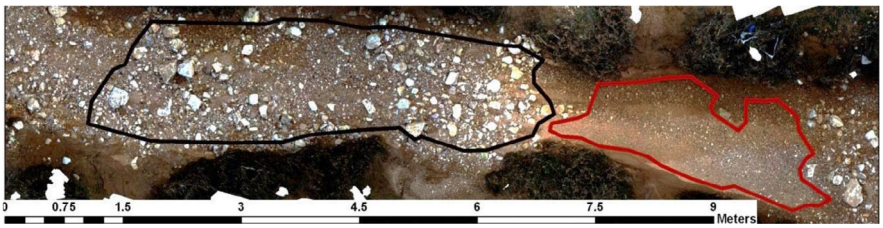

FIGURE 3 Example of clear-cut morphological differences between the bedforms on the Yatir channel bed. The bar is outlined by a black line and the flat by a red line. Flow is from left to right.

TABLE 1 Percentiles and parameters of representative grain size (*D*) distributions based on Wolman sampling and of DEM-derived height (*q*) distributions of the undisturbed (T_{-1}) channel bedforms.

	D_{05} q_{05}	D_{16} q_{16}	D_{50} q_{50}	D_{84} q_{84}	D_{95} q_{95}	average	SD (σ)
Percentile/parameter				**mm**			
bars (height)	30	37	48	62	78	50	15
flats (height)	11	13	16	19	22	16	3
bars (grain size)	12	15	30	58	94	42	34
flats (grain size)	11	13	17	27	53	24	17

the aligned elevation grid represent areas where the elevation value on the sloped surface is greater than the elevation value on the original elevation grid.

Roughness values were calculated based on the minimum value in each height grid (Pearson et al., 2017). This method has been applied in a similar manner in studies based on roughness estimation with a ground laser scanner (Storz-Peretz & Laronne, 2013). Statistical analysis was undertaken on the height values representing each cell of the aligned raster (Bertin et al., 2017, 2018; do Prado et al., 2025). Data processing was performed in R Studio software to examine the distribution of heights (Table S2) in a selected macroform. Percentiles such as q_{05}, q_{16}, q_{50}, q_{84}, q_{95}, the mean and standard deviation (STDV) were extracted from the distribution and characteristic values were defined for each macroform.

Many attempts were made to develop a tool that would automatically and objectively distinguish different roughness phenomena, *viz*. bars and flats, based on various statistical parameters (such as those deployed by Mair et al., 2022). As each flat includes some large clasts and bars include some patches of fine-grained sediment, the automatic processing did not yield satisfactory results. So, instead, this step was performed manually. Four of the researchers independently delimited macroforms on orthophotos, estimating their outlines by eye. The results were then compared and found to be remarkably similar, the boundaries lying within centimetres (at field scale) in all cases (Figure 3). The robustness and reproducibility of the method allowed us to demarcate the macroforms as they developed during the 2-year period of observations.

FIGURE 4 Downstream view of the Yatir study reach as a mini excavator was mixing the channel bed material, thereby destroying the sedimentary and topographic character of the flat-bar sequence.

The surface grain size distributions of three of the bars, three of the flats and one transitional area were determined in the field using a Wolman grid (Wolman, 1954) and by sieving bulk samples. These were complemented by determination of the local frequency distributions of heights derived from DEMs (Table 1), rather than by measurements of the longest axis of selected grains (*cf*. Garefalakis et al., 2023). Although the values at percentiles and parameters of surface heights are not identical to those of the surface grain sizes, they co-vary (Table 1).

Once the initial surveys and sampling were complete, the channel bed was excavated to a depth of 0.5 m using a mini excavator (Figure 4). The sediment was thoroughly mixed, and then reintroduced as a homogenized mixture, or as homogenized as could be feasibly achieved. The surface was graded so that it was planar. A survey of the post-mixing longitudinal profile revealed some minor prominences, which were eliminated by localized adjustments of the bed surface. The long profile was then re-surveyed, and this was repeated after all but one of the flow events occurring in the following two rain seasons.

Mixing of the channel bed inevitably decreased its bulk density (Table S1). The degree of change was assessed by comparing values derived for the undisturbed bed with those at three well-spaced locations in the study reach after treatment using the large sand cone method (ASTM D1556–07).

Flood water-stage was monitored by a Levelogger 5 (Solinst) that has a non-vented pressure sensor with a full-scale accuracy of ±0.05%. Water depth was established after compensating for monitored changes in atmospheric pressure. Stage hydrographs allowed us to assess the effect of water depth and flow duration on channel bed changes.

TABLE 2 Flow events in Nahal Yatir during the study period.

runoff season	event #	event date	peak stage m	event duration h	# of peaks*
2016–2017	1	14–15/12/2016	0.53	41	2
	2	19–20/12/2016	0.23	23	1
	3	27/1/2017	0.40	58	4
	4	31/1/2017	0.52	38	2
	5	12–17/2/2017	0.38	132	9
2017–2018	6	1–2/1/2018	0.19	9	2
	7	5–6/1/2018	0.52	23	3
	8	19–20/1/2018	0.53	31	3
	9	27–28/1/2018	0.49	38	3
	10	29/1/2018	0.31	12	1

*These arise from either changes in rain intensity or staggered arrival of tributary flows as convective rain cells traverse the catchment.

Data collection in semi-desert channels is particularly challenging because of high sediment flux (Alexandrov et al., 2009) and the way that these compromise monitoring sensors. So, during 2016–17, mud had collected unnoticed at the bottom of the stilling well carrying the pressure transducers, and its very low permeability led to slow release of water towards the end of each event, resulting in a slightly convex-up bulge in the record at the end of flow recession. This was rectified during the second year by ensuring that the sensor was kept clear of deposited fine-grained sediment so that the stilling well was able to drain as flow receded.

4 | RESULTS

Altogether, ten flow events occurred in the Yatir during the two-year study period (Table 2). For these brief and discrete periods of flow, peak water depth ranged from 0.19 to 0.53 m, the number of intra-flood peaks from 1 to 9 and duration ranged from 9 to 132 h.

At least one peak stage in each of the 10 events was sufficient to generate bedload transport, which, in the Yatir, typically occurs at and above a critical water depth of 10 cm (Reid, Laronne, & Powell, 1995). Flash flood hydrographs are 'peaky'; the rise in stage is very steep (Figure 5); and, although flow recession is prolonged relative to the time of rise, overall its duration is generally short.

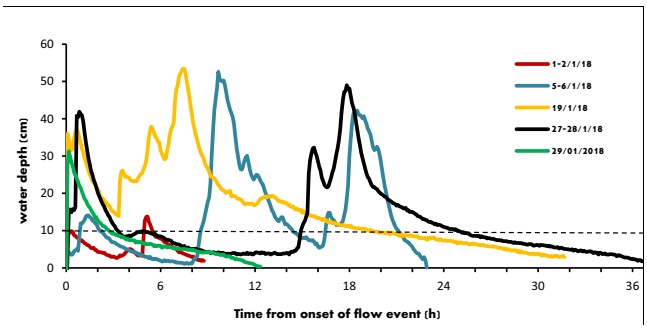

FIGURE 5 Nahal Yatir stage hydrographs during winter 2017–2018. The dashed line represents the threshold of bedload motion.

The longitudinal profile of the study reach was altered considerably by the mixing of the bed material. Not only did the treatment destroy the regular macroform sequence and generate a relatively planar surface (Figure 4), but the bed surface increased in height on average by 11 cm (Figure 6). This dilation was reflected in the dry bulk density (D_b) of the sediment (Table S2; Supplement 1). After mixing, D_b was, on average, 85% of that typical of the undisturbed channel bed, indicating an expected increase in surface elevation of 9 cm. The looseness of the bed material will, of course, have influenced its entrainment dynamics, at least during the first few post-treatment flow events.

The original, undisturbed, channel bed was characterized by large downstream differences in local longitudinal slope. The average slope of the bars was 1.7%, contrasting strongly with an average negative slope of −0.1% for the flats (Figure 6). After mixing, the slope of the reach was, by design, almost planar. With the passage of successive flash floods, the profile became less planar and more uneven as the macroforms started to re-establish (Figure 6; Table 3).

The differentiation of grain size between bars and flats was very pronounced in the original surface, as reflected in differences in grain size and grain-scale roughness (Figures 3 and 7). This is parameterized by the standard deviation of surface heights, which, for the bars, was 15 mm and, for the flats, 3 mm. It is also reflected in the differences in

TABLE 3 Evolution of the average longitudinal slope of macroforms of each type identified before bed material disturbance (T_{-1}) and after each subsequent flashflood (T_1 through T_9). The reach slope remained unchanged at 0.01.

slope, %								
	T_{-1}	T_1	T_2	T_5	T_6	T_7	T_8	T_9
Bar	1.7	1.4	1.1	1.5	1.5	2.0	1.5	1.8
Flat	−0.1	0.3	0.9	−0.3	0.7	−0.5	0.0	−0.1

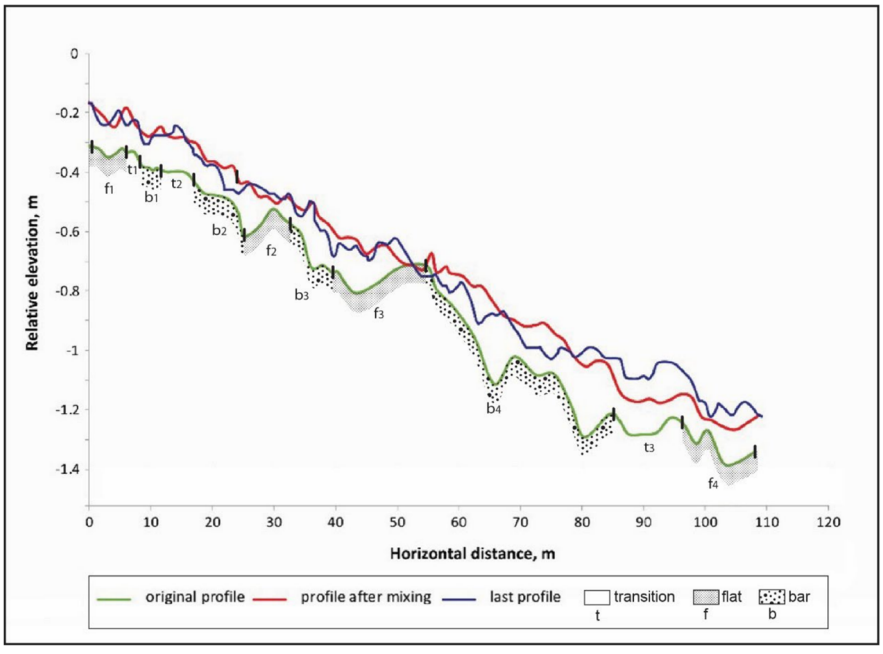

FIGURE 6 Longitudinal profiles of the Yatir study reach prior to artificial disturbance, after mixing and at the end of the second winter runoff season. The overall longitudinal slope of the study reach remained unchanged at 0.01.

mean height of clasts on each type bedform: the value for bars was 50 mm, while that for flats was 16 mm (Table 2; Supplement 2S). The smooth, planar nature of the flats is reflected in having no protruding pebbles (maximum D_{90} ≤ 20 mm; Figure 7), except the occasional overpassing clast stranded by flow recession (see, e.g., the flat in Figure 3). This was the condition prior to bed disturbance. The differentiation of roughness was also typical of bars and flats as they re-formed (T_1 through T_9).

Once the bed had been mixed, these differences were eliminated. This had to be evaluated by eye from the close-range aerial imagery, as there was no opportunity to monitor the bed at T_0 prior to the T_1 flood event. So, as mentioned above, for the sites that had been bars before treatment, the standard deviation of surface heights was 15 mm and the equivalent for flats was 3 mm (Figure 7). After the passage of eight of the ten floods, these values evolved to become 20 mm and 4 mm, respectively.

The entire process of textural restoration is clearly exemplified by the temporal change in roughness. The initial post-treatment roughness is characterized in Figure 7a. Change began as early as the first flow event (Figure 7b) and was very obvious after the 5th (Figure 7c), i.e. by the end of the first flood season. Figure 7d illustrates the frequency distributions of grain-scale heights at the end of the second flood season, from which it can be seen that, for all practical purposes, the differentiation of bars and flats is almost identical to the original state of the bed (Figure 7a).

Figure 8 further illustrates the post-treatment restoration process. This portion of the channel was, before treatment, a well-developed flat, flanked up- and downstream by coarser bars (Figure 8A, T_{-1}). The surface of the homogenized bed material (T_0) is captured in Figure 8B. A finer-grained patch became evident in mid-segment after the 2nd flow event (Figure 8C), increasing in area after succeeding events (Figures 8D, E, F) and giving rise to the spatial restoration of the bar-flat sequence that had been evident before treatment (Figure 8A).

A more complex restoration process is exemplified in Figure 9. This original coarse-grained bar (Figure 9A, T_{-1}) was mixed to form a

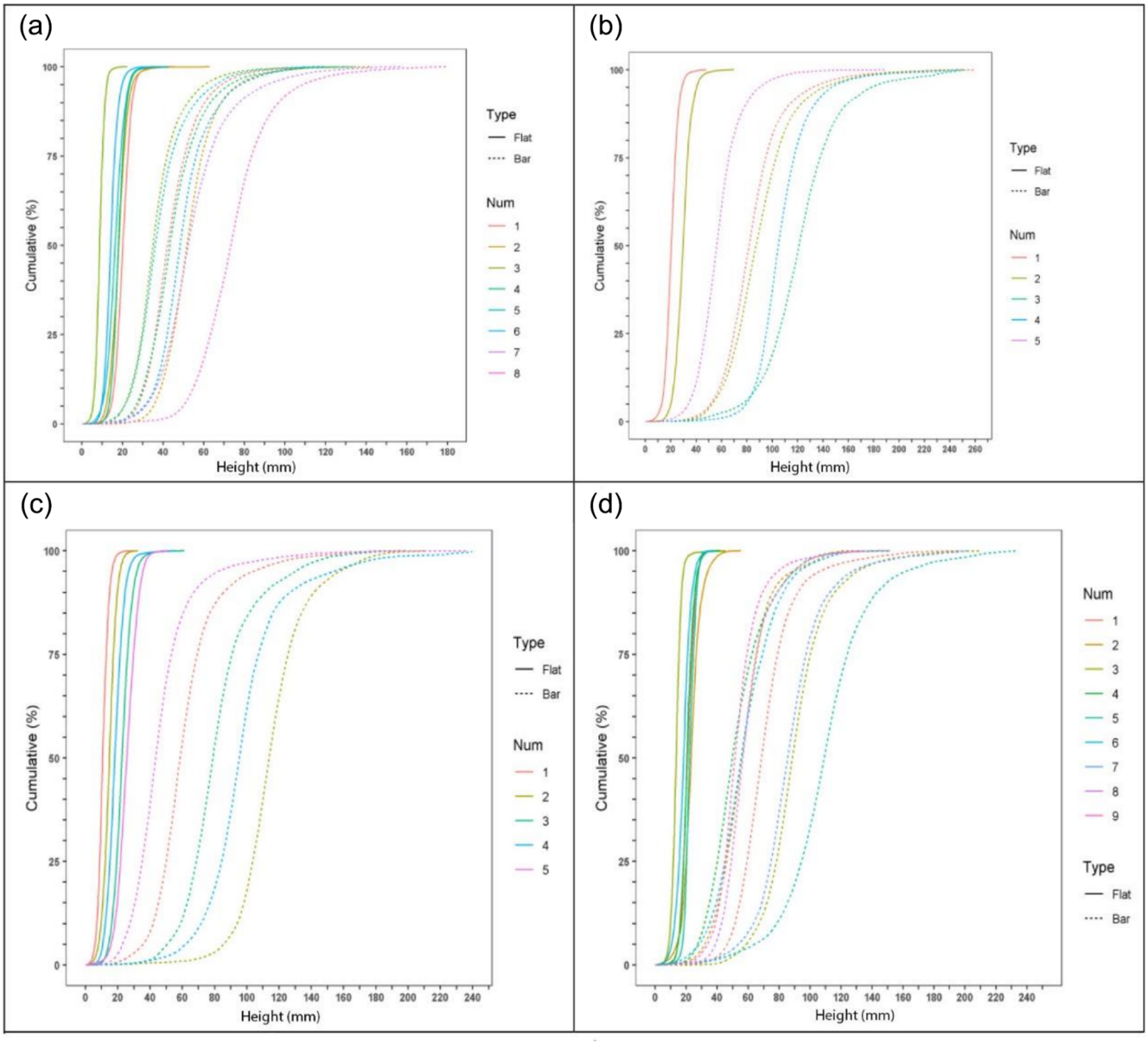

FIGURE 7 Frequency distributions of Yatir grain-scale heights of type-macroforms: (a) before bed material homogenization at T_{-1}; (b) post first flood at T_1; (c) post 5th flood at T_5; and (d) post 9th and 10th floods at T_9. The colours represent the designated number of bars or flats.

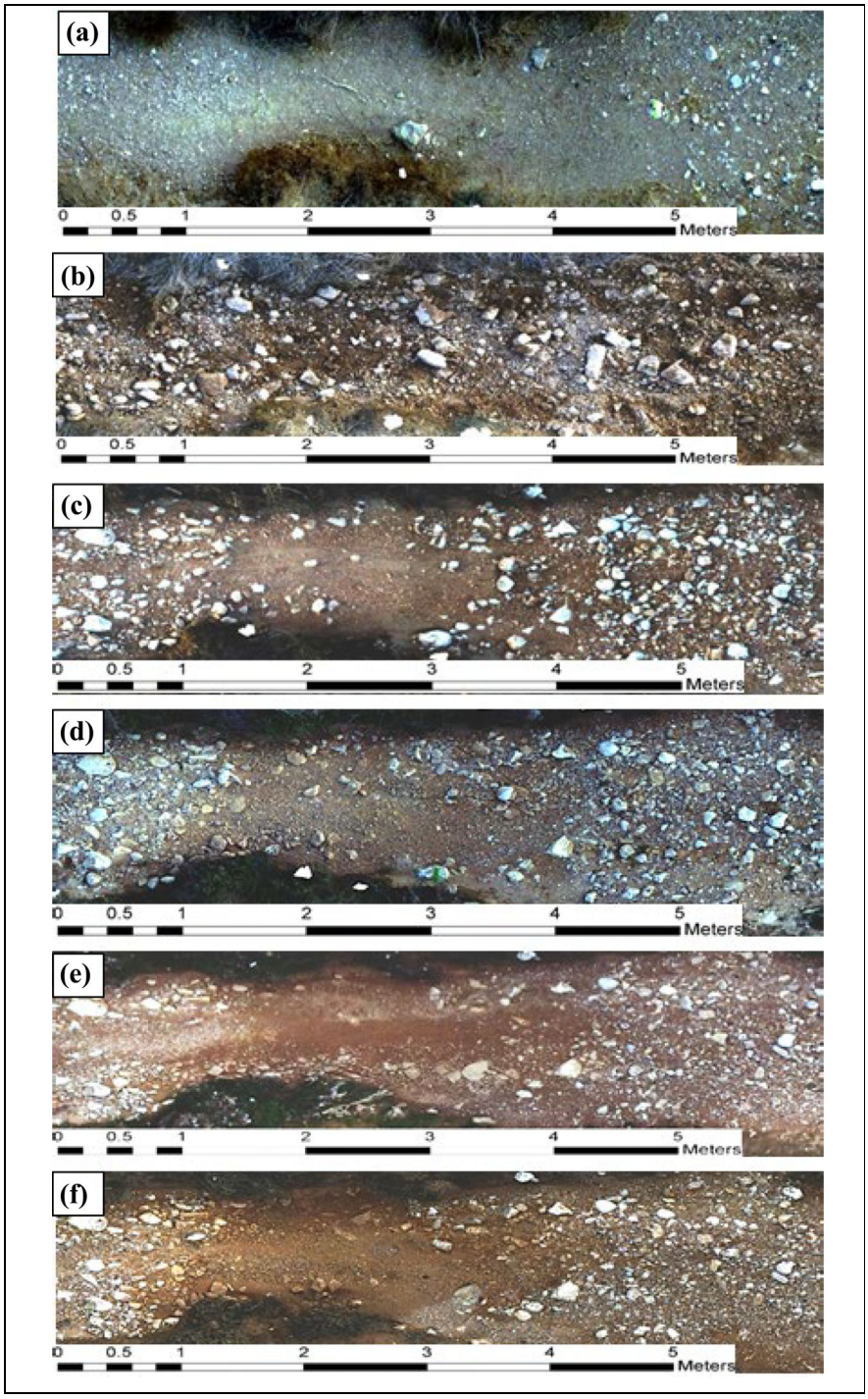

FIGURE 8 Example of the changes in the channel bed during the study period: (A) *flat* in the original channel bed (T_{-1}); (B) after mixing the channel bed (T_0); (C) channel bed after the second flood event (T_2); (D) channel bed after the fifth flood event; (E) channel bed after the seventh flood event; and (F) channel bed after the tenth flood event. Flow is left to right.

homogeneous, finer-grained surface (Figure 9B, T_0). Subsequently, finer-grained particles were deposited (Figure 9C, D). The outcome, at least during the run of observations, was a well-defined bar formed upstream of a flat (Figure 9E, F).

5 | DISCUSSION

While allowing for the random placement of the survey staff in relation to surface clasts during each survey, the post-treatment long-profile and that established at the conclusion of the study are remarkably similar in general elevation (Figure 6). This we judge to be testimony to the fact that any bedform restoration was a result of selective sediment transport and deposition and that progressive, differential consolidation of the bed material during the period of observation was not significant and can be ruled out as a factor affecting the long-profile.

Indeed, a close inspection of the sequential images of the bed (Figures 8 and 9) reveals detail that is pertinent to the role of sediment transport as the primary restoration process. A glance at the image of the treated sediment surface shown in Figure 8B suggests that the general orientation of the a-axis of individual coarse clasts of cobble size, which have an axial ratio b/a generally ≤ 0.5 is disorganized. Some of these clasts lie with their a-axes athwart the streamlines whilst others are sub-parallel. In fact, an analysis shows that, after artificial homogenization of the bed material, the orientations of these clasts ranges over 180 degrees, diverging from the longitudinal axis of the channel by up to ± 90 degrees, with only 16% aligned within ±

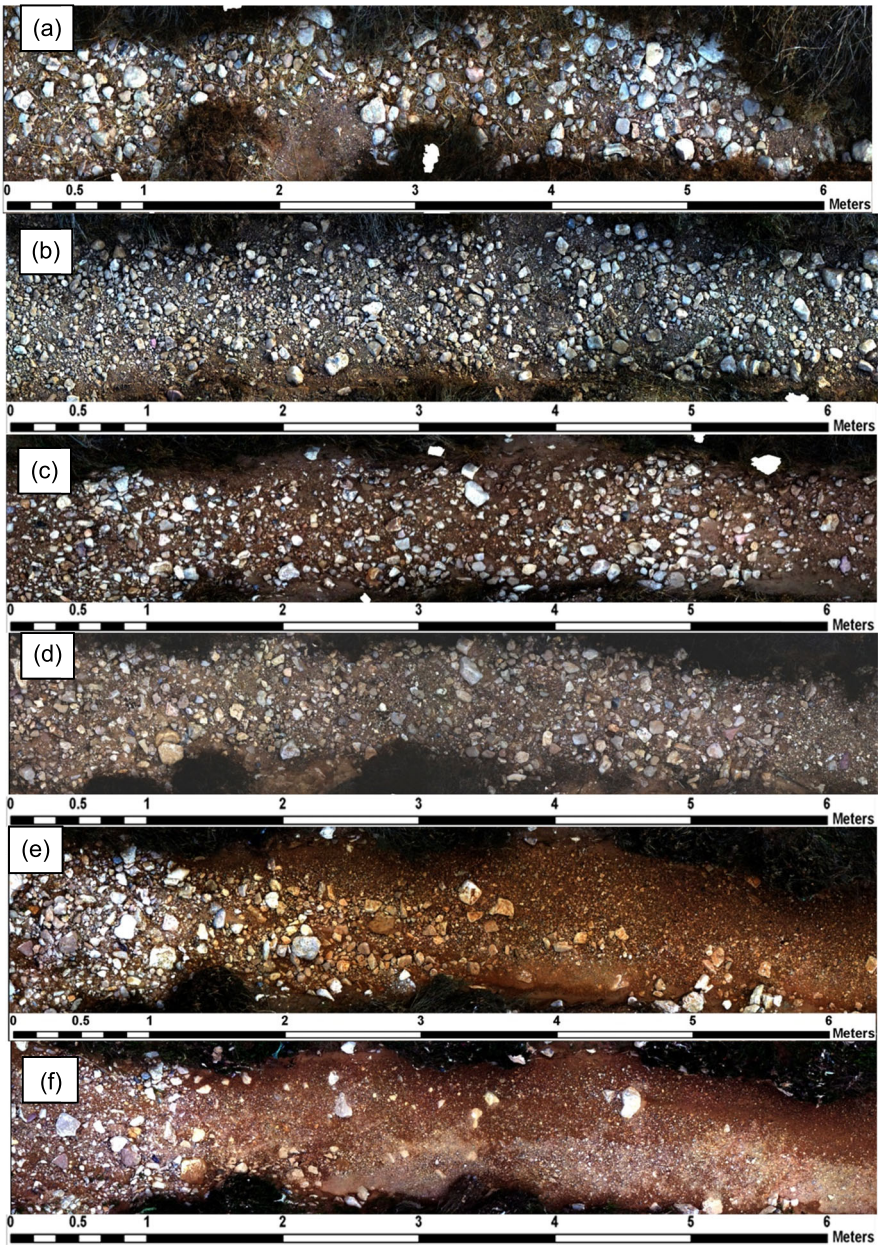

FIGURE 9 Example of the changes in the channel bed during the study period: (A) *bar* in the original channel bed (T_{-1}); (B) after mixing the channel bed (T_0); (C) channel bed after the second flood event (T_2); (D) channel bed after the fifth flood event; (E) channel bed after the seventh flood event; and (F) channel bed after the tenth flood event. Flow is left to right.

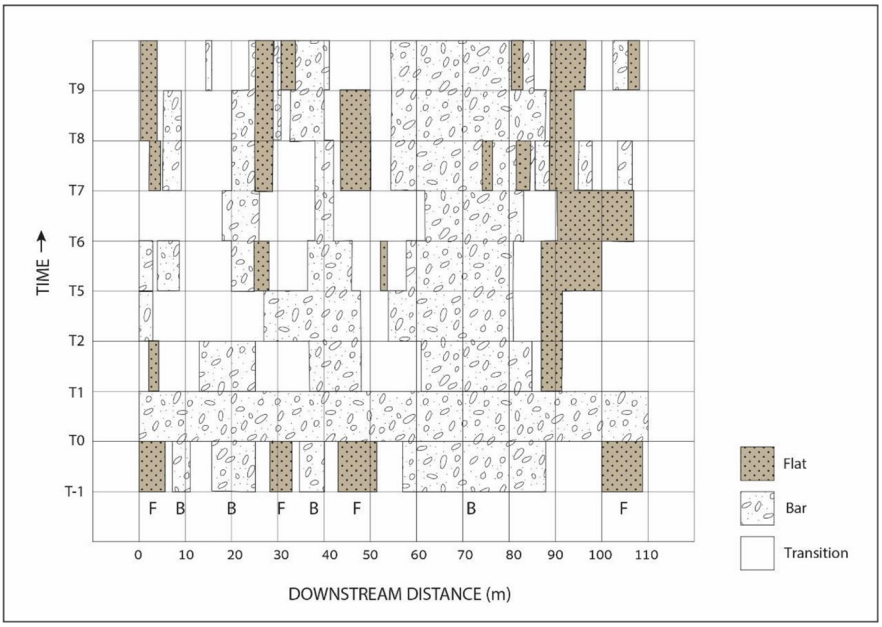

FIGURE 10 The location of macroforms: T_{-1} pre-treatment bed material; T_0 bed material homogenization; T_1 through T_9 subsequent successive flow events. The non-stippled zones of this spatio-temporal diagram have textural character transitional between bars and flats.

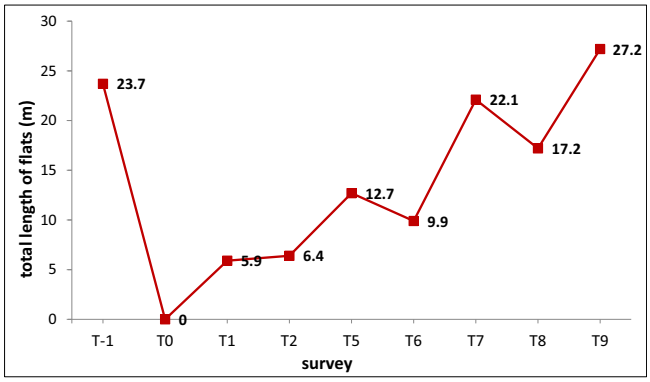

FIGURE 11 The original aggregated length of flats in the Yatir study reach (T_{-1}), their disappearance upon homogenizing the bed (T_0) and their gradual re-establishment after each successive flood (T_1 through T_9).

10 degrees. However, after flood events 1 (Q_p stage = 0.53 m) and 2 (Q_p stage = 0.23 m), the a-axes of these clasts are almost all orientated stream-wise (Figure 8C). This change is complete by the end of the observation period and an examination of Figure 8F shows that, after the 10th flash flood, all such clasts lie within ± 10 degrees of the primary streamline. Were shear stresses only marginally capable of moving these larger clasts, one might expect their a-axes to lie orthogonal to the streamline (Johansson, 1963). The fact that they align with the flow indicates that stresses and, hence, bedload flux (largely consisting of smaller clasts) were large, consistent both with previous studies of flux in the same channel (Reid, Powell, et al., 1995) and with the demonstration in neighbouring Nahal Eshtemoa that equal mobility of clasts of all sizes is achieved at sub-bankfull stage during flash floods in these upland ephemeral rivers (Powell et al., 2001).

The location of the two type-macroforms appears to depend, at least in part, on local hydraulic geometry, and, most obviously, to co-vary with channel width: bars are predominantly associated with narrow sections while flats occur where the channel is wider (Powell et al., 2012; *cf*. Nelson et al., 2015). Interestingly, when compared with the study reach average (1.71 m), the width of the Yatir channel is narrower (1.37 m) in the 55–85 m segment. It is, therefore, no surprise that an elongate bar existed in this segment prior to bed reworking and that bars tended to reform in this segment after the first post-treatment flow event (Figure 10). Such narrower segments of the channel are often where 'obstacle clasts' or 'keystones' tend to occur, trapping coarser clasts (Curran, 2012; Lamarre & Roy, 2008; Reid et al., 1992; Zimmerman & Church, 2001).

Though macroform topography and texture were destroyed by artificially mixing the bed material, it is evident that even the first flow event induced some flats to begin to re-form, occupying, at this stage, 5% of the study reach, but that they continued to grow through successive events until, at survey T_9, the length of channel occupied (27%) matched that of the undisturbed original (24%; Figure 11). As time progressed, the disposition of each type-bedform appeared to bear an increasing similarity with that of the natural, undisturbed bed (T_{-1}, Figure 10). However, self-evidently, the spatial pattern at the end of our observations (T_9) is not identical. It is likely that the process of restoration was incomplete by T_9, and perhaps this should not be surprising. After all, the spasmodic runoff regime of this semi-arid environment meant that the duration of flow in excess of the threshold of bedload motion was only about 50 hours in two years, 0.3% of the period of our observations.

A mechanism of grain size segregation is key to understanding the formation and existence of alternating bar-flat macroforms, and we develop this in our companion paper (Massera et al., 2025).

6 | CONCLUSIONS

The bed material in a straight reach of a coarse-grained natural channel was thoroughly mixed to a depth of 0.5 m. In its undisturbed state, it had exhibited alternating, channel-wide bars and flats, a bedform pattern that is typical of upland, ephemeral, gravel-bed rivers. The treatment obliterated the macroforms in terms of both texture - and thus bedform-scale roughness - and longitudinal slope. The reach was then monitored over two years using repeated SfM photography and total station surveys to assess the impact of successive flash floods and to gauge whether the macroforms re-formed and, if so, where and at what rate.

Our conclusions are that the macroforms begin to re-establish even after a few moderate flow events, facilitated by the high bedload flux that has previously been shown to be characteristic of upland ephemeral streams. Small patches of finer-grained flats appeared to be formed immediately by the first, post-treatment, flow event. Coarser-grained bars tended to re-establish in narrower segments of the channel and flats in wider segments, the overall pattern bearing resemblance to the original, undisturbed channel bed. The longitudinal slopes of the re-forming bars were greater than or equal to the average reach slope, whereas those of emerging flats were significantly less and, in places, negative, mimicking the original, undisturbed bed. It is apparent that the driver of both the formation and maintenance of alternating bar-flat sequences is contingent on bedload transport, a link which we develop as an integral element of a numerical model in a companion paper (Massera et al., 2025).

ACKNOWLEDGEMENTS

We thank Ofer Sholker Kona of the Shima-Bsor Drainage Authority for technical assistance, Daniel, Avigayil and Geva for field assistance and Roni Livnon for drafting the Figures. We extend our thanks to Luca Mao, Review Editor and three anonymous reviewers for their insightful and helpful comments. These have allowed us to greatly improve the paper.

CONFLICT OF INTEREST STATEMENT

We declare no conflict of interest.

DATA AVAILABILITY STATEMENT

The data that support the findings of this study are available on request from the corresponding author. The data are not publicly available due to privacy or ethical restrictions.

PERMISSION TO REPRODUCE MATERIAL FROM OTHER SOURCES

We give permission to reproduce any of the material in this submission with appropriate reference to this publication.

ORCID

Jonathan B. Laronne https://orcid.org/0000-0002-2889-9316
D. Mark Powell https://orcid.org/0000-0002-7667-6272
Michael Dorman https://orcid.org/0000-0001-6450-8047
Annunziato Siviglia https://orcid.org/0000-0003-1192-1596
Marco Tubino https://orcid.org/0000-0001-7298-7818
Gabriele Massera https://orcid.org/0009-0003-0672-1239
Ian Reid https://orcid.org/0000-0002-8589-0940

REFERENCES

Alexandrov, Y., Cohen, H., Laronne, J.B. & Reid, I. (2009) Suspended sediment load, bed load, and dissolved load yields from a semiarid drainage basin: A 15-year study. *Water Resources Research*, 45(8), W08408. Available from: https://doi.org/10.1029/2008WR007314

Assouline, S. & Ben-Hur, M. (2006) Effects of rainfall intensity and slope gradient on the dynamic of interrill erosion during soil surface sealing. *Catena*, 66(3), 211–220. Available from: https://doi.org/10.1016/j.catena.2006.02.005

Barzilai, R. (2012) *Repeating channel bedforms in ephemeral coarse-grained alluvial rivers: their character, distribution and influence on bedload flux and texture*. Unpublished PhD dissertation. Beer Sheva, Israel: Ben Gurion University of the Negev.

Ben-Hur, M., Shainberg, I., Keren, R. & Gal, M. (1985) Effect of water quality and drying on soil crust properties. *Soil Science Society of America J.*, 49(1), 191–196. Available from: https://doi.org/10.2136/sssaj1985.03615995004900010038x

Bertin, S., Groom, J. & Friedrich, H. (2017) Isolating roughness scales of gravel-bed patches. *Water Resources Research*, 53(8), 6841–6856. Available from: https://doi.org/10.1002/2016WR020205

Bertin S.J., Groom, J. & Friedrich, H. (2018) Grain and bedform roughness properties isolated from gravel-patch DEMs. RiverFlow 2018. E3S Web of Conferences 40, 04005.https://doi.org/10.1051/e3sconf/20184004005

Buffington, J.M. & Montgomery, D.R. (1999) Effects of sediment supply on surface textures of gravel bed rivers. *Water Resources Research*, 35(11), 3523–3530. Available from: https://doi.org/10.1029/1999WR900232

Callander, R.A. (1969) Instability and river channels. *Journal of Fluid Mechanics*, 36(3), 465–480. Available from: https://doi.org/10.1017/S0022112069001765

Carrivick, J. L., Smith, M. W. & Quincey, D. J. (2016) *Structure from Motion in the Geosciences*. New York: Wiley Blackwell, https://doi.org/10.1002/9781118895818

Chin, A. (2002) The periodic nature of step-pool mountain streams. *American Journal of Science*, 302(2), 144–167. Available from: https://doi.org/10.2475/ajs.302.2.144

Chin, A. & Wohl, E. (2005) Toward a theory for step pools in stream channels. *Progress in Physical Geography*, 29(3), 275–296. Available from: https://doi.org/10.1191/0309133305pp449ra

Clifford, N.J. (1993) Formation of riffle–pool sequences: field evidence for an autogenetic process. *Sedimentary Geology*, 85(1-4), 39–51. Available from: https://doi.org/10.1016/0037-0738(93)90074-F

Colombini, M., Seminara, G. & Tubino, M. (1987) Finite-amplitude alternate bars. *Journal of Fluid Mechanics*, 181, 213–232. Available from: https://doi.org/10.1017/S0022112087002064

Curran, J.C. (2012) Examining individual step stability within step-pool sequences. In: Church, M., Biron, P. & Roy, A.G. (Eds.) *Gravel Bed Rivers 7: Processes, Tools, Environments*. Chichester: Wiley-Blackwell, pp. 378–385 https://doi.org/10.1002/9781119952497.ch27

Danin, A., Arbel, A. & Levy, N. (1998) *The Carta Atlas of the fauna and flora of the Holyland*. Jerusalem: Carta.

Dietrich, J.T. (2014) *Applications of structure-from-motion photogrammetry to fluvial geomorphology*. Unpublished PhD Dissertation. Eugene, Oregon: University of Oregon.

do Prado, A.H., Mair, D., Garefalakis P., Silveira, B.C., Whittaker, A.C. & Schlunegger, F. (2025) The influence of grain size sorting on the roughness parametrization of gravel riverbeds. *Geomorphology*, 471, 109565. Available from: https://doi.org/10.1016/j.geomorph.2024.109565

Engelund, F. (1970) Instability of erodible beds. *Journal of Fluid Mechanics*, 42(2), 225–244. Available from: https://doi.org/10.1017/S0022112070001210

Garefalakis, P., do Prado, A.H., Mair, D., Douillet G.A., Nyffenegger, F. & Schluneggr, F. (2023) Comparison of three grain size measuring methods applied to coarse-grained gravel deposits. *Sedimentary Geology*, 446, 106340. Available from: https://doi.org/10.1016/j.sedgeo.2023.106340

Golly, A., Turowski, J.M., Badoux, A. & Hovius, N. (2019) Testing models of step formation against observations of channel steps in a steep mountain stream. *Earth Surface Processes and Landforms*, 44(7), 1390–1406. Available from: https://doi.org/10.1002/esp.4582

Hassan, M.A. (2005) Characteristics of gravel bars in ephemeral streams. *Journal of Sedimentary Research*, 75(1), 29–42. Available from: https://doi.org/10.2110/jsr.2005.004

Hassan, M.A., Egozi, R. & Parker, G. (2006) Experiments on the effect of hydrograph characteristics on vertical grain sorting in gravel bed rivers. *Water Resources Research*, 42(9), W09408. Available from: https://doi.org/10.1029/2005WR004707

Hayashi, T. (1970) Formation of dunes and antidunes in open channels. *Journal of the Hydraulics Division*, 96(2), 357–366. Available from: https://doi.org/10.1061/JYCEAJ.0002324

Johansson, C.-E. (1963) Orientation of pebbles in running water. *A laboratory study. Geografisca Annaler*, 45(2/3), 85–112. Available from: https://doi.org/10.2307/520386

Kahana, R., Ziv, B., Enzel, Y. & Dayan, U. (2002) Synoptic climatology of major floods in the Negev Desert, Israel. *International Journal of Climatology*, 22(7), 867–882. Available from: https://doi.org/10.1002/joc.766

Kennedy, J.F. (1963) The mechanics of dunes and antidunes in erodible-bed channels. *Journal of Fluid Mechanics*, 16(4), 521–544. Available from: https://doi.org/10.1017/S0022112063000975

Kuhnle, R.A., Horton, J.K., Bennett, S.J. & Best, J.L. (2006) Bed forms in bimodal sand–gravel sediments: laboratory and field analysis. *Sedimentology*, 53(3), 631–654. Available from: https://doi.org/10.1111/j.1365-3091.2005.00765.x

Lamarre, H. & Roy, A.G. (2008) A field experiment on the development of sedimentary structures in a gravel-bed river. *Earth Surface Processes and Landforms*, 33(7), 1064–1081. Available from: https://doi.org/10.1002/esp.1602

Laronne, J.B., Reid, I., Yitshak, Y. & Frostick, L.E. (1994) The non-layering of gravel streambeds under ephemeral flood regimes. *Journal of Hydrology*, 159(1-4), 353–363. Available from: https://doi.org/10.1016/0022-1694(94)90266-6

Lisle, T.E. & Hilton, S. (1999) Fine bed material in pools of natural gravel bed channels. *Water Resources Research.*, 35(4), 1291–1304.

Mair, D., Do Prado, A.H., Garefalakis, P., Lechmann, A., Whittaker, A. & Schlunegger, F. (2022) Grain size of fluvial gravel bars from close-range UAV imagery–uncertainty in segmentation-based data. *Earth Surface Dynamics Discussions*, 10(5), 1–33. Available from: https://esurf.copernicus.org/articles/10/953/2022/, https://doi.org/10.5194/esurf-10-953-2022

Massera, G., Siviglia, A., Laronne, J.B., Reid, I., Powell, D.M., Cohen, T., et al. (2025) Formation of repeating bar-flat bedforms in ephemeral gravel bed channels: 2. *bridging mathematical modelling and field observations*. *Earth Surface Processes and Landforms*, 50(13), e70184. Available from: https://doi.org/10.1002/esp.70184

Montgomery, D.R. & Buffington, J.M. (1997) Channel-reach morphology in mountain drainage basins. *Geological Society of America Bulletin*, 109(5), 596–611. Available from: https://doi.org/10.1130/0016-7606(1997)109<0596:CRMIMD>2.3.CO;2

Nelson, P.A., Brew, A.K. & Morgan, J.A. (2015) Morphodynamic response of a variable-width channel to changes in sediment supply. *Water Resources Research.*, 51(7), 5717–5734. Available from: https://doi.org/10.1002/2014WR016806

Parker, G. (1976) On the cause and characteristic scales of meandering and braiding in rivers. *Journal of Fluid Mechanics*, 76(3), 457–480. Available from: https://doi.org/10.1017/S0022112076000748

Pearson, E., Smith, M.W., Klaar, M.J. & Brown, L.E. (2017) Can high resolution 3D topographic surveys provide reliable grain size estimates in gravel bed rivers? *Geomorphology*, 293, 143–155. Available from: https://doi.org/10.1016/j.geomorph.2017.05.015

Powell, D.M., Laronne, J.B., Reid, I. & Barzilai, R. (2012) The bed morphology of upland single-thread channels in semi-arid environments: evidence of repeating bedforms and their wider implications for gravel-bed rivers. *Earth Surface Processes & Landforms*, 37(7), 741–753. Available from: https://doi.org/10.1002/esp.3199

Powell, D.M., Reid, I. & Laronne, J.B. (2001) Evolution of bedload grain-size distribution with increasing flow strength and the effect of flow duration on the calibre of bedload sediment yield in ephemeral gravel-bed rivers. *Water Resources Research*, 37(5), 1463–1474. Available from: https://doi.org/10.1029/2000WR900342

Recking, A., Frey, P., Paquier, A. & Belleudy, P. (2009) An experimental investigation of mechanisms involved in bed load sheet production and migration. *Journal of Geophysical Research-Earth Surface*, 114(F3), F03010. Available from: https://doi.org/10.1029/2008JF000990

Reid, I., Frostick, L.E. & Brayshaw, A.C. (1992) Microform roughness elements and the selective entrainment and entrapment of particles in gravel-bed rivers. In: Billi, P., *et al*. (Eds.) *Dynamics of gravel-bed rivers*. Chichester: John Wiley & Sons, pp. 253–266.

Reid, I. & Laronne, J.B. (1995) Bedload sediment transport in an ephemeral stream and a comparison with seasonal and perennial counterparts. *Water Resources Research*, 31(3), 773–781. Available from: https://doi.org/10.1029/94WR02233

Reid, I., Laronne, J.B. & Powell, D.M. (1995) The Nahal Yatir bedload database: sediment dynamics in a gravel-bed ephemeral stream. *Earth Surface Processes and Landforms*, 20(9), 845–857. Available from: https://doi.org/10.1002/esp.3290200910

Reid, I., Laronne, J.B. & Powell, D.M. (1998) Flashflood and bedload dynamics of desert gravel-bed streams. *Hydrological Processes*, 12(4), 543–557. Available from: https://doi.org/10.1002/(SICI)1099-1085(19980330)12:4<543::AID-HYP593>3.0.CO;2-C

Reid, I., Powell, D.M., Laronne, J.B. & Garcia, C. (1995) Flash floods in desert rivers. *Earth in Space*, 7(39), 7–8. Available from: https://doi.org/10.1029/94EO01076

Richards, K.J. (1980) The formation of ripples and dunes on an erodible bed. *Journal of Fluid Mechanics*, 99(3), 597–618. Available from: https://doi.org/10.1017/S002211208000078X

Richards, K.S. (1976) The morphology of riffle-pool sequences. *Earth Surface Processes*, 1(1), 71–88. Available from: https://doi.org/10.1002/esp.3290010108

Shentsis, I., Laronne, J.B. & Alpert, P. (2012) Red Sea trough floods in the Negev, Israel (1964-2007). *Hydrological Sciences Journal*, 57(1), 42–51. Available from: https://doi.org/10.1080/02626667.2011.636922

Smith, M.W. & Vericat, D. (2015) From experimental plots to experimental landscapes: topography, erosion and deposition in sub-humid badlands from structure from motion photogrammetry. *Earth Surface Processes and Landforms*, 40(12), 1656–1671. Available from: https://doi.org/10.1002/esp.3747

Sneh, A., and Avni, Y. (2008) Geological map of Israel 1:50,000, Eshtemoa, Sheet 15–1. Geological Survey of Israel.

Stark, K., Cadol, D., Leary, K. & Laronne, J.B. (2025) Persistently high bedload flux in ephemeral channels. *Geomorphica*, 1(1), 1–15. Available from: https://doi.org/10.59236/geomorphica.v1i1

Storz-Peretz Y. & Laronne, J.B. (2013) Morpho-textural characterization of dryland braided channels. *Bulletin Geological Society of America*, 125 (9/10), 1599–1617. https://doi.org/10.1130/B30773.1

Storz-Peretz, Y. & Laronne, J.B. (2018) The morpho-textural signature of large bedforms in gravel bed channels of various patterns. *Hydrological Processes*, 1-19(5), 617–635. Available from: https://doi.org/10.1002/hyp.11437

Storz-Peretz, Y., Laronne, J.B., Surian, N. & Lucia, A. (2016) Flow recession as a driver of the morpho-texture of braided streams. *Earth Surface Processes and Landforms*, 41(6), 754–770. Available from: https://doi.org/10.1002/esp.3861

Taylor, J.R. (1997) *Introduction to error analysis: the study of uncertainties in physical measurements*. 2nd ed. Sausalito, CA, USA: University of Science Books.

Venditti, J.G., Nelson, P.A., Bradley, R.W., Haught, D. and Gitto, A.B. (2017) Bedforms, Structures, Patches, and Sediment Supply in Gravel-Bed Rivers. pp 439-466, Chapter 16 In Gravel-Bed Rivers: Processes and Disasters (eds D. Tsutsumi and J.B. Laronne). https://doi.org/10.1002/9781118971437.ch16

Westoby, M.J., Brasington, J., Glasser, N.F., Hambrey, M.J. & Reynolds, J.M. (2012) 'Structure-from-Motion' photogrammetry: A low-cost, effective tool for geoscience applications. *Geomorphology*, 179, 300–314. Available from: https://doi.org/10.1016/j.geomorph.2012.08.021

Whiting, P.J., Dietrich, W.E., Leopold, L.B., Drake, T.G. & Shreve, R.L. (1988) Bedload sheets in heterogeneous sediment. *Geology*, 16(2), 105–108. Available from: https://doi.org/10.1130/0091-7613(1988)016<0105:BSIHS>2.3.CO;2

Whittaker, J.G. & Jaeggi, M.N. (1982) Origin of step-pool systems in mountain streams. *Journal of Hydraulic Engineering*, 108(6), 758–773. Available from: https://doi.org/10.1061/JYCEAJ.0005873

Wolman, M.G. (1954) A method of sampling coarse river-bed material. *United States Geological Survey Professional Paper*, 35(6), 951–956.

Yair, A. & Kossovsky, A. (2002) Climate and surface properties: hydrological response of small and semi-arid watersheds. *Geomorphology*, 42(1–2), 43–57. Available from: https://doi.org/10.1016/S0169-555X(01)00072-1

Zimmerman, A. & Church, M. (2001) Channel morphology, gradient profiles and bed stresses during flood in a step-pool channel. *Geomorphology*, 40(3-4), 311–327. Available from: https://doi.org/10.1016/S0169-555X(01)00057-5

SUPPORTING INFORMATION

Additional supporting information can be found online in the Supporting Information section at the end of this article.

How to cite this article: Laronne, J.B., Cohen, T., Powell, D.M., Dorman, M., Siviglia, A., Tubino, M. et al. (2025) Formation of repeating bar-flat bedforms in ephemeral gravel bed channels: 1. Field observations. *Earth Surface Processes and Landforms*, 50(15), e70203. Available from: https://doi.org/10.1002/esp.70203